

Controlling Style and Semantics in Weakly-Supervised Image Generation

Dario Pavllo Aurelien Lucchi Thomas Hofmann
 Department of Computer Science
 ETH Zürich

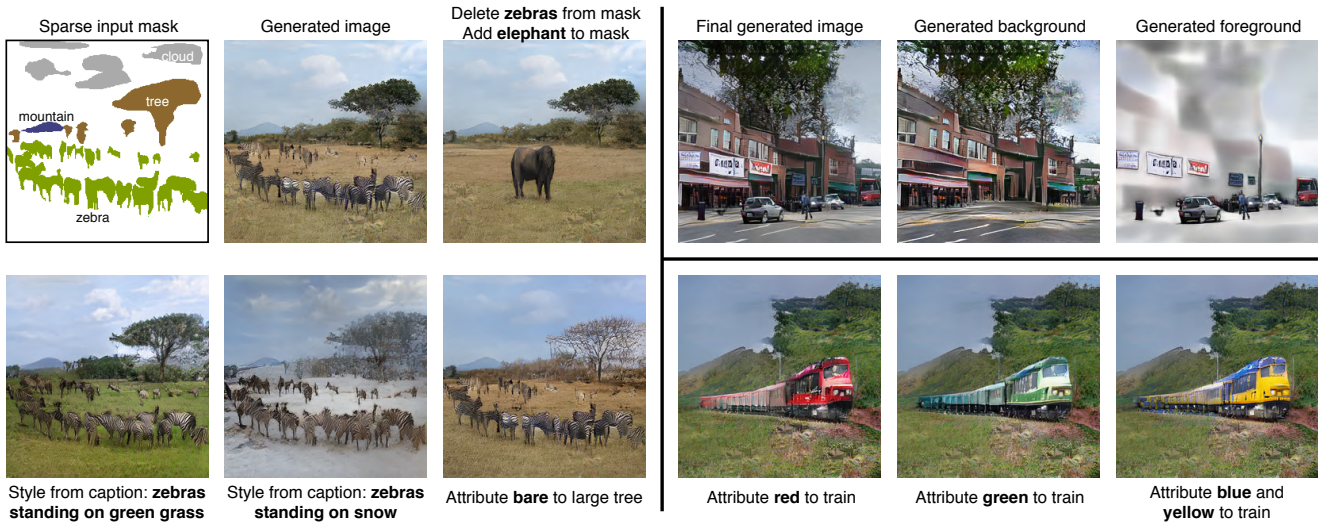


Figure 1: Our approach makes it possible to control the style of the scene and its objects through high-level attributes or textual descriptions. It also enables image manipulation through the mask, including moving, deleting, or adding object instances. The decomposition of the background and foreground (top-right corner) facilitates local changes in a scene.

Abstract

We propose a weakly-supervised approach for conditional image generation of complex scenes where a user has fine control over objects appearing in the scene. We exploit sparse semantic maps to control object shapes and classes, as well as textual descriptions or attributes to control both local and global style. To further augment the controllability of the scene, we propose a two-step generation scheme that decomposes background and foreground. The label maps used to train our model are produced by a large-vocabulary object detector, which enables access to unlabeled sets of data and provides structured instance information. In such a setting, we report better FID scores compared to a fully-supervised setting where the model is trained on ground-truth semantic maps. We also showcase the ability of our model to manipulate a scene on complex datasets such as COCO and Visual Genome.

1. Introduction

Deep generative models such as VAEs [22] and GANs [9] have made it possible to learn complex distributions over various types of data, including images or text. For images, recent technical advances [13, 19, 27, 28, 45, 1] have enabled GANs to produce realistically-looking images for a large number of classes. However, these models often do not provide high-level control over image characteristics such as appearance, shape, texture, or color, and they fail to accurately model multiple (or compound) objects in a scene, thus limiting their practical applications.

A related line of research aims at disentangling factors of variation during the generation process [20]. While these approaches can produce images with varied styles by injecting noise at different levels, the style factors are learned without any oversight, leaving the user with a loose handle on the generation process. Furthermore, their applicability has only been demonstrated to single-domain images (e.g. faces, cars or birds). Some conditional approaches allow to control the style of an image using either attributes [42, 12]

or natural language [46, 47, 41], but again, these methods only show compelling results on single-domain datasets.

One key aspect in generative modeling is the amount of required semantic information: i) *weak conditioning* (e.g. a sentence that describes a scene) makes the task underconstrained and harder to learn, potentially resulting in incoherent images on complex datasets. On the other hand, ii) *rich semantic information* (in the extreme case, full segmentation masks) yields the best generative quality, but requires more effort from an artist or dataset annotator. The applications of such richly-conditioned models are numerous, including art, animation, image manipulation, and realistic texturing of video games. Existing works in this category [4, 30, 16, 40, 29] typically require hand-labeled segmentation masks with per-pixel class annotations. Unfortunately, this is not flexible enough for downstream applications such as image manipulation, where the artist is faced with the burden of modifying the semantic mask in a coherent way. Common transformations such as moving, deleting, or replacing an object require instance information (which is not always available) and a strategy to properly fill-in the background. Moreover, these models present little-to-no high-level control over the style of an image and its objects.

Our work combines the merits of both weak conditioning with strong semantic information by relying on both mask-based generation – using a variant we call *sparse masks* – as well as text-based generation – which can be used to control the style of the objects contained in the scene as well as its global aspects. Fig. 1 conceptualizes our idea. Our approach uses a large-vocabulary object detector to obtain annotations, which are then used to train a generative model in a weakly-supervised fashion. The input masks are sparse and retain instance information – making them easy to manipulate – and can be inferred from images or videos.

Fig. 2 highlights another issue with current generative models: local changes made to an object (such as moving or deleting) can affect the scene globally due to the learned correlations between objects. While these entangled representations are useful to maximize scene coherence, they do not allow the user to modify a local part of a scene without affecting the rest. To this end, our approach relies on a multi-step generation process where we first generate a *background image* and then we generate foreground objects conditioned on the former. The background image can also be frozen when manipulating the foreground objects.

Finally, we evaluate our approach on COCO [25, 5, 2] and Visual Genome [24], and show that our weakly-supervised setting can achieve better FID scores [13] than fully-supervised counterparts, while being more controllable and scalable to large unlabeled datasets.

In summary, our contributions are:

- We propose weakly-supervised training using *sparse masks*: semantic masks inferred from an object detec-

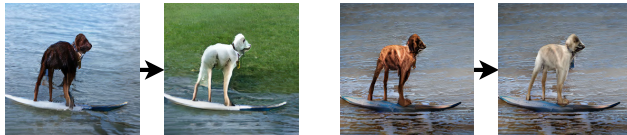


Figure 2: **Left:** in a single-generator model, local changes (in this case, changing the color of the dog to white) affect the scene globally due to learned correlations. **Right:** in a two-step model, we can freeze the result of the first step (background) while manipulating the instances in the scene.

tor. These are easy to draw or manipulate, and allow the model to be trained on large unlabeled datasets.

- We show that our setting achieves better FID scores than existing models trained in fully-supervised settings due to our ability to better model fine details.
- We propose an *entangled* multi-step generation scheme that separates background and foreground generation without sacrificing visual quality, and which facilitates local manipulations.
- An approach for controlling the style of the scene and its instances, either using high-level attributes or natural language with an attention mechanism.
- We will soon release our code.

2. Related work

The recent success of GAN models has triggered a lot of interest for conditional image synthesis where images are being generated from categorical labels [27, 28, 45, 1], text [31, 46, 47, 41], semantic maps [16, 40, 29], or conditioning images from other domains [49, 16].

Image generation from semantic maps. In this setting, a semantic segmentation map is translated into a natural image. Non-adversarial approaches are typically based on perceptual losses [4, 30], whereas GAN architectures are based on patch-based discriminators [16], progressive growing [40, 19], and conditional batch normalization where the semantic map is fed to the model at different resolutions [29]. Due to its stability and compelling results, we decided to base our architecture on [29]. Most approaches are trained on hand-labeled masks (limiting their application in the wild), but [29] shows one example where the model is weakly supervised on masks inferred using a semantic segmentation model [3]. Our model is also weakly supervised, but instead of a semantic segmentation model we use an object detector – which allows us to maintain instance information during manipulations, and results in *sparse masks*. While early work focused on class semantics, recent methods support some degree of style control. E.g. [40] trains an instance autoencoder and allows the user to choose a latent code from among a set of modes, whereas [29] trains a VAE to control the global style of a generated image by copying the style of a *guide* image. Both these methods, however,

do not provide fine-grained style control (e.g. changing the color of an object to *red*). Another recent trend consists in generating images from structured layouts, which are transformed into semantic maps as an intermediate step to facilitate the task. In this regard, there is work on generation from bounding-box layouts [48, 14] and scene graphs [17].

Semantic control. Existing approaches do not allow for easy manipulation of the semantic map because they present no interface for encoding existing images. In principle, it is possible to train a weakly-supervised model on maps inferred from a semantic segmentation model, as [29] does for landscapes. However, manipulations are still challenging because instance information is not available. Furthermore, since the label masks are *dense*, even simple transformations such as deleting or moving an object would create holes in the semantic map that need to be adjusted by the artist. *Dense* masks also make the task too constrained with respect to background aspects of the scene (e.g. sky, land, weather), which leaves less room for style control.

Text-based generation. Some recent models condition the generative process on text data. These are often based on autoregressive architectures [32] and GANs [31, 46, 47, 41]. Learning to generate images from text using GANs is known to be difficult due to the task being unconstrained. In order to ease the training process, [46, 47] propose a two-stage architecture named *StackGAN*. To avoid the instability associated with training a language model jointly with a GAN, they use a pretrained sentence encoder [23] that encodes a caption into a fixed-length vector which is then fed to the model. More advanced architectures such as *AttnGAN* [41] use an attention mechanism which we discuss in one of the next paragraphs. These approaches show interesting results on single-domain datasets (birds, flowers, etc.) but are less effective on complex datasets such as *COCO* [25] due to the intrinsic difficulty of generating coherent scenes from text alone. Some works [18, 44] have demonstrated that generative models can benefit from taking as input multiple diverse textual descriptions per image. Finally, we are not aware of any prior work that conditions the generative process on *both* text and semantic maps (our setting).

Multi-step generation. Approaches such as [43, 36] aim at disentangling background and foreground generation. While fully-unsupervised disentanglement is provably impossible [26], it is still achievable through some form of inductive bias – either in the model architecture or in the loss function. While [43] uses spatial transformers to achieve separation, [36] uses object bounding boxes. Both methods show compelling results on single-domain datasets that depict a centered object, but are not directly applicable to more challenging datasets. In our setting, we are not interested in full disentanglement (i.e. we do not assume independence between background and foreground), but merely in

separating the two steps while keeping them interpretable. Our model still exploits correlations among classes to maximize visual quality, and is applied to datasets with complex scenes. Finally, there has also been work on interactive generation using dialogue [8, 6, 34].

Attention models in GANs. For unconditional models (or models conditioned on simple class labels), self-attention GANs [45, 1] use a visual-visual attention to improve spatial coherence. For generation from text, [41] employ sentence-visual attention coupled with an LSTM encoder, but only in the generator. Instead of adding attention in the discriminator, the caption is enforced through a supervised loss based on features extracted from a pretrained Inception [38] network. In our case, we use a new form of attention (*sentence-semantic*) which is applied to semantic maps instead of convolutional feature maps, and whose computational cost is independent of the image resolution. It is applied both to the generator and the discriminator, and on the sentence side it features a transformer-based [39] encoder.

3. Approach

3.1. Framework

Our main interest is conditional image generation of complex scenes where a user has fine control over the objects appearing in the scene. Prior work has focused on generating objects from ground-truth masks [49, 16, 40, 29] or on generating outdoor scenes based on simple hand-drawn masks [29]. While the former approach requires a significant labeling effort, the latter is not directly suitable for complex datasets such as *COCO*-Stuff [2], whose images consist of a large number of classes with complex (hard to draw) shapes. We address these problems by introducing a new model that is conditioned on sparse masks – to control object shapes and classes – and on text/attributes to control style and textures. This gives the ability to a user to produce realistic scenes through a variety of image manipulations (such as moving, scaling or deleting an instance, adding an instance from another image or from a database of shapes) as well as style manipulations controlled using either high-level attributes on individual instances (e.g. *red*, *green*, *wet*, *shiny*) or using text that refers to objects as well as global context (e.g. “a red car at night”). In the latter case, visual-textual correlations are not explicitly defined but are learned in an unsupervised way.

Sparse masks. Instead of training a model on precise segmentation masks, as in [16, 40, 29], we use a mask generated automatically from a large-vocabulary object detector. Although this process introduces some noise, it also has the benefit of providing information about each instance (which may not always be available otherwise), including parts of objects which would require significant manual effort to label in a new dataset. In general, our set of classes comprises

countable objects (person, car, etc.), parts of objects (light, window, door, etc.), as well as uncountable classes (grass, water, snow), which are typically referred to as “stuff” in the COCO terminology [2]. For the latter category, an object detector can still provide useful sparse information about the background, while keeping the model autonomous to fill-in the gaps. We describe the details of our object detection setup in [sec. 4.2](#).

Two-step generation. In the absence of constraints, conditional models learn class correlations observed in the training data. For instance, while dogs typically stand on green grass, zebras stand on yellow grass. While this feature is useful for maximizing scene coherence, it is undesirable when only a local change in the image is wanted. We observed similar global effects on other local transformations, such as moving an object or changing its attributes, and generally speaking, small perturbations of the input can result in large variations of the output. We show such an example in [Fig. 2](#). To tackle this issue, we propose a variant of our architecture which we call *two-step* model and which consists of two concatenated generators ([Fig. 3](#)). The first step (generator G_1) is responsible for generating a *background* image, whereas the second step (generator G_2) generates a *foreground* image conditioned on the background image. The definition of what constitutes background and foreground is arbitrary: our choice is to separate by class: static/uncountable objects (e.g. buildings, roads, grass, and other surfaces) are assigned to *background*, and moving/countable objects are assigned to *foreground*. Some classes can switch roles depending on the parent class, e.g. *window* is *background* by default, but it becomes *foreground* if it is a child of a foreground object such as a car.

When applying a local transformation to a foreground object, the background can conveniently be frozen to avoid global changes. As a side benefit, this also results in a lower computational cost to regenerate an image. Unlike work on disentanglement [43, 36] which enforces that the background is independent of the foreground without necessarily optimizing for visual quality, our goal is to enforce separation while maximizing qualitative results. In our setting, G_1 is exposed to both background and foreground objects, but its architecture is designed in a way that foreground information is not rendered, but only used to induce a bias in the background (see [sec. 3.2](#)).

Attributes and captions. Our method allows the user to control the style of individual instances using high-level attributes. These attributes refer to appearance factors such as colors (e.g. white, black, red), materials (wood, glass), and even modifiers that are specific to classes (leafless, snowy), but not shape or size, since these two are determined by the mask. An object can also combine multiple attributes (e.g. black and white) or have none – in this case, the generator

would pick a predefined mode. This setup gives the user a lot of flexibility to manipulate a scene, since the attributes do not need to be specified for every object.

Alternatively, one can consider conditioning style using natural language. This has the benefit of being more expressive, and allows the user to control global aspects of the scene (e.g. time of the day, weather, landscape) in addition to instance-specific aspects. While this kind of conditioning is harder to learn than plain attributes, in [sec. 3.2](#) we introduce a new attention model that shows compelling results without excessively increasing the model complexity.

3.2. Architecture

We build our architecture upon *SPADE* [29], a conditional GAN architecture that has demonstrated stability in a wide range of scenarios. In the original formulation, the semantic map is fed to the generator at increasing spatial resolutions using conditional batch normalization. They use a multi-scale discriminator [40] where the semantic map is concatenated to the input. Additionally, they augment the adversarial loss with a perceptual loss using a pretrained VGG network [35] and a feature matching loss in the discriminator [40].

One-step model. Since this model ([Fig. 3](#), left) serves as a baseline, we keep its architecture as close as possible to the reference model of [29]. We propose to insert the required information about attributes/captions in this architecture by modifying the input layer and the conditional batch normalization layers (*SPADE* blocks) of the generator, which is where semantic information is fed to the model. We name these *augmented SPADE* blocks. We apply the same change to the input layer of the discriminators.

Augmented SPADE block. In the original SPADE [29], the class mask (i.e. semantic map) is converted to a one-hot representation and convolved using 3×3 kernels with 128 output channels. The resulting feature map is passed through a ReLU non-linearity and convolved again to produce two feature maps γ and β , respectively, the conditional batch normalization gain and bias. The normalization is then computed as $\mathbf{y} = \text{BN}(\mathbf{x}) \odot (1 + \gamma) + \beta$, where $\text{BN}(\mathbf{x})$ is the parameter-free batch normalization.

While 3×3 convolutions on one-hot masks are adequate when applied to a small set of classes, they result in too many parameters when applied to a large number of classes (our setting). Therefore, we replace the 3×3 convolutions on one-hot masks with a 64-dim. pixel-wise embedding layer followed by 3×3 convolutions. We apply the same principle to the first layer of the generator and discriminators. To add style information, we concatenate another 64-dim. representation to the class embedding (pixel-wise). We explain how we derive these representations in the next two paragraphs.

Conditioning on attributes. For attributes, we adopt a *bag-*

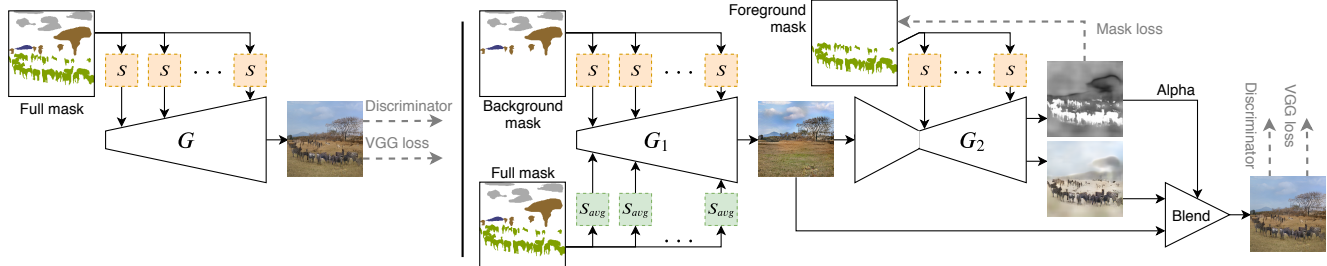


Figure 3: **Left:** One-step model (augmented SPADE). **Right:** two-step model. The background generator G_1 takes as input a *background mask* (processed by S blocks) and the full mask (processed by S_{avg} blocks, where positional information is removed). The foreground generator takes as input the output of G_1 and a *foreground mask*. Finally, the two outputs are alpha-blended. For convenience, we do not show attributes/text in this figure.

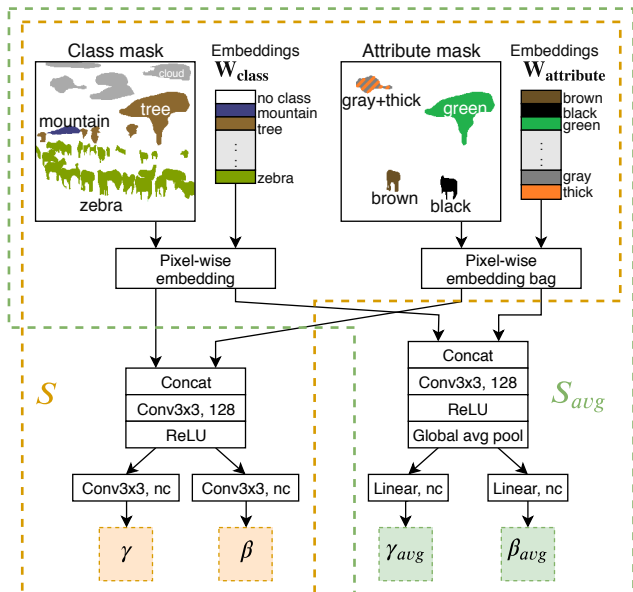


Figure 4: Our SPADE block augmented with attributes. Class and attribute embeddings are concatenated and processed to generate the conditional batch normalization gain and bias. In the attribute mask, embeddings take the shape of the instance to which they refer. In G_1 of the two-step model, where S and S_{avg} are both used, the embedding weights are shared.

of-embeddings approach where we learn a 64-dim. embedding for each possible attribute, and all attribute embeddings assigned to an instance are simply broadcast to the shape of the instance, summed together, and concatenated to the class embedding. Fig. 4 (S block) depicts this process. To implement this efficiently, we create a multi-hot *attribute mask* (1 in the locations corresponding to the attributes assigned to the instance, 0 elsewhere) and feed it through a 1×1 convolutional layer with N_{attr} input channels and 64 output channels. Attribute embeddings are shared among classes and are not class-specific. This helps the model generalize better (e.g. colors such as “white” apply both to vehicles and animals), and unseen combinations

(e.g. leafless person) are simply ignored by the generator without side effects.

Conditioning on text. While previous work has used fixed-length vector representations [46, 47] or one-layer attention models coupled with RNNs [41], the diversity of our scenes led us to use a more powerful encoder entirely based on self-attention [39]. We encode the image caption using a pretrained BERT_{base} model [7], which consists of 12 attention layers and 110M parameters. It is unreasonable to attach such a model to a GAN and fine-tune it, both due to excessive memory requirements and due to potential instabilities. Instead, we freeze the pretrained model and encode the sentence, extract its hidden representation before the last layer (i.e. second-to-last), and train a custom multi-head attention layer for our task. This approach, which is also suggested by [7], has proven successful on a variety of NLP downstream tasks, especially when these involve small datasets or limited vocabularies. Furthermore, instead of storing the language model in memory, we simply pre-compute the sentence representations and cache them.

Next, we describe the design of our trainable attention layer (Fig. 5). Our attention mechanism is different from sentence-visual attention [41], where attention is directly applied to convolutional feature maps inside the generator. Instead, we propose a form of sentence-semantic attention which is computationally efficient, interpretable, and modular. It can be concatenated to existing SPADE layers in the same way as we concatenate attributes. Compared to sentence-visual attention, whose cost is $\mathcal{O}(nd^2)$ (where n is the sentence length and $d \times d$ is the feature map resolution), our method has a cost of $\mathcal{O}(nc)$ (where c is the number of classes), i.e. it is independent of the image resolution. We construct a set of c queries (i.e. one for each class) of size $h = 64$ (where h is the attention head size). We feed the hidden representations of each token of the sentence to two linear layers, one for the *keys* and one for the *values*. Finally, we compute a scaled dot-product attention [39], which yields a set of c values. To allow the SPADE block to attend to multiple parts of the sentence, we use

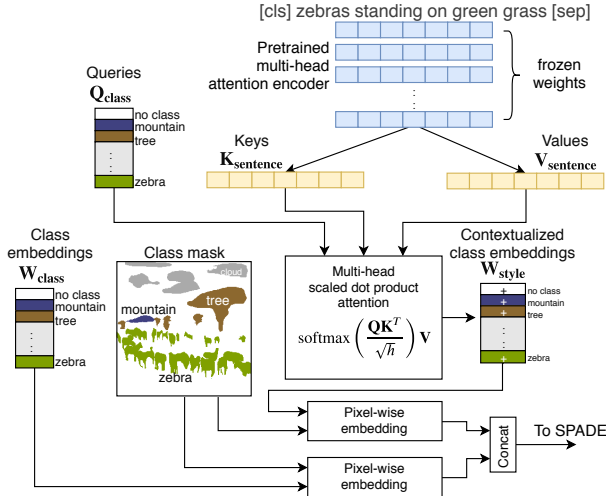


Figure 5: Attention mechanism for conditioning style via text. The sentence (of length $n = 7$ including delimiters) is fed to a pretrained attention encoder, and each token is transformed into a key and a value using two trainable linear layers. The queries are learned for each class, and evaluating the attention function results in a set of contextualized class embeddings that are concatenated to the regular semantic embeddings.

12 attention heads, whose output values are concatenated and further transformed through a linear layer. This process can be thought of as generating *contextualized class embeddings*, i.e. class embeddings customized according to the sentence. For instance, given a semantic map that depicts a car and the caption “a red car and a person”, the query corresponding to the visual class *car* would most likely attend to “red car”, and the corresponding value will induce a bias in the model to add redness to the position of the car. Finally, the *contextualized class embeddings* are applied to the semantic mask via pixel-wise matrix multiplication with one-hot vectors, and concatenated to the *class embeddings* in the same way as attributes. In the current formulation, this approach is unable to differentiate between instances of the same class. We propose a possible mitigation in [sec. 5](#).

Two-step model. This model consists of two concatenated generators. G_1 generates the background, i.e. it models $p(x_{bg})$, whereas G_2 generates the foreground conditioned on the background, i.e. $p(x_{fg}|x_{bg})$. One notable difficulty in training such a model is that background images are never observed in the training set (we only observe the final image), therefore we cannot use an intermediate discriminator for G_1 . Instead, we use a single, final discriminator and design the architecture in a way that the gradient of the discriminator (plus auxiliary losses) is redirected to the correct generator. A natural choice is *alpha blending*, which is also used in [\[43, 36\]](#) for different reasons. Intuitively, G_2 generates an RGB foreground image plus a transparency mask (*alpha* channel), and the final image is obtained by pasting

the foreground onto the background via linear blending:

$$x_{final} = x_{bg} \cdot (1 - \alpha_{fg}) + x_{fg} \cdot \alpha_{fg},$$

where x_{final} , x_{bg} , and x_{fg} are RGB images, and α_{fg} is a 1-channel image bounded in $[0, 1]$. Readers familiar with highway networks [\[37\]](#) might notice a similarity to this approach in terms of gradients dynamics. If $\alpha_{fg} = 1$, the gradient is completely redirected to x_{fg} while if $\alpha_{fg} = 0$, the gradient is redirected to x_{bg} . This scheme allows us to train both generators in an end-to-end fashion using a single discriminator, and we can also preserve auxiliary losses (VGG loss, feature matching loss) which [\[29\]](#) has shown to be very important for convergence. To incentivize separation between classes as defined in [sec. 3.1](#), we provide supervision on α_{fg} using a binary cross-entropy loss, and decay this term over time (see [sec. 4.2](#)).

In G_2 we use the same augmented SPADE blocks as the ones used in the one-step model (S block), which take the *foreground mask* as input. Since G_1 must exploit foreground information without rendering it, we devise a further variation of SPADE that consists of two branches: (i) the first branch (S block) takes the *background mask* as input and processes it as usual to produce the batch normalization gain γ and bias β . (ii) the second branch (S_{avg} block, [Fig. 4](#)) takes the full mask as input (background plus foreground), processes it, and applies global average pooling to the feature map to remove information about localization. This way, the foreground information is only used to bias the generator and cannot be rendered at precise spatial locations. After pooling, it outputs γ_{avg} and β_{avg} . (iii) The final conditional batch normalization is computed as

$$y = \text{BN}(x) \odot (1 + \gamma + \gamma_{avg}) + \beta + \beta_{avg}$$

Note that, if G_1 took the full mask as input without information reduction, it would render visible “holes” in the output image due to gradients never reaching the foreground zones of the mask, which is exactly what we are trying to avoid. Finally, the discriminator D takes the full mask as input (background plus foreground). In the [App. A.1](#) we provide further low-level details about our architectures.

4. Experiments

4.1. Setup and datasets

For consistency with [\[29\]](#), we always evaluate our model on the COCO-Stuff validation set [\[2\]](#), but we train on a variety of training sets:

COCO-Stuff (COCO2017) [\[25, 2\]](#) contains 118k training images with captions [\[5\]](#). We train with and without captions. COCO-Stuff extends COCO2017 with ground-truth semantic maps, but for our purposes the two datasets are equivalent since we do not exploit ground-truth masks.

Visual Genome (VG) [\[24\]](#) contains 108k images that partially overlap with COCO ($\approx 50\%$). VG does not have a

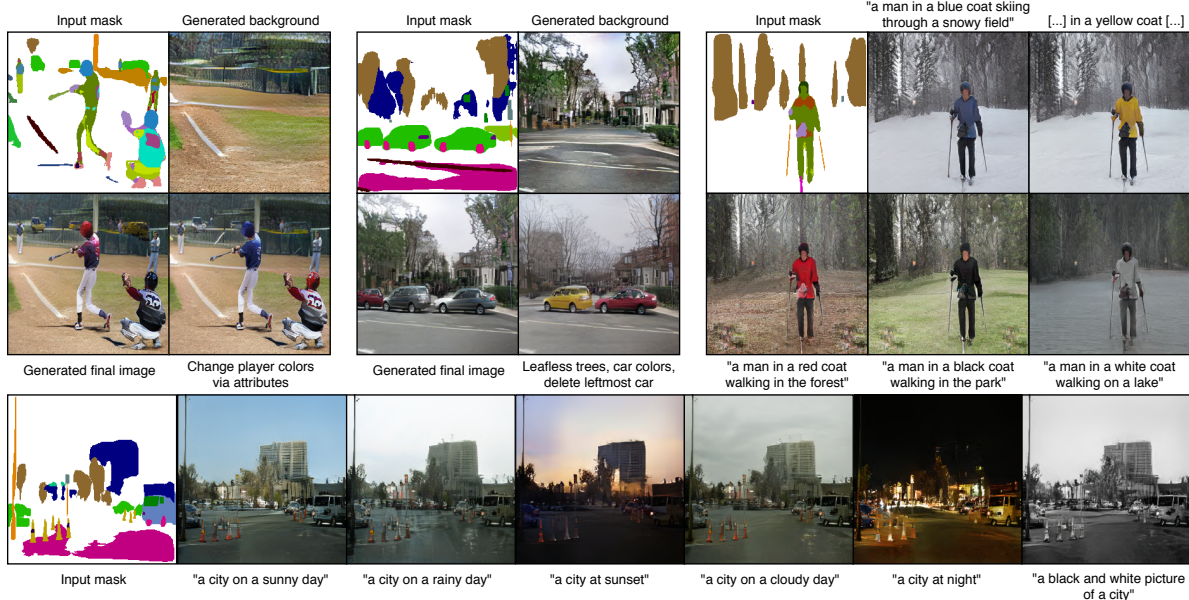


Figure 6: Qualitative results (256×256 resolution). **Top-left** and **top-middle**: two-step generation with manipulation of attributes and instances. **Top-right**: manipulating style (both context and instances) via text. **Bottom**: manipulating global style via text.

default train/test split, therefore we leave out 10% of the dataset to use as a development set (IDs ending with 9), and use the rest as a training set from which we remove images that overlap with the COCO-Stuff validation set. We extract the attributes from the scene graphs.

Visual Genome augmented (VG+) VG augmented with the 123k images from the COCO unlabeled set. The total size is 217k images after removing exact duplicates. The goal is to evaluate how well our method scales to large unlabeled datasets. We train without attributes and captions.

For all experiments, we evaluate the *Fréchet Inception Distance* (FID) [13]. We report our results (qualitative and quantitative) in sec. 4.3. Furthermore, we provide precise implementation details of the FID in the Appendix A.2 as well as additional qualitative results in A.3.

4.2. Implementation details

Semantic maps. To construct the input semantic maps, we use the semi-supervised implementation of Mask R-CNN [11, 33] proposed by [15]. It is trained on bounding boxes from Visual Genome (3000 classes) and segmentation masks from COCO (80 classes), and learns to segment classes for which there are no ground-truth masks. We discard the least frequent classes, and, since some VG concepts overlap (e.g. car, vehicle) leading to spurious detections, we merge these classes and end up with a total of $c = 280$ classes (plus a special class for “no class”). We set the threshold of the object detector to 0.2, and further refine the predictions by running a class-agnostic non-maximum-suppression (NMS) step on the detections whose mask intersection-over-union (IoU) is greater than 0.7. We

also construct a transformation hierarchy to link children to their parents in the semantic map (e.g. headlight of a car), further details in Appendix A.1. We select the 256 most frequent attributes, manually excluding those that refer to shapes (e.g. *short*, *square*).

Training. Unless specified otherwise, our settings are the same as [29], including the image resolution which is 256×256 . In all experiments, we train on 8 Pascal GPUs for 100 epochs, and we start decaying the learning rate to 0 after the 50th epoch in a linear fashion. We use a batch size of 32 for the *one-step* model and 24 for the *two-step* model, which is the largest batch size that we can fit into memory, and we keep synchronized batch normalization enabled. Training takes approximately one week for the one-step model, and two weeks for the two-step model. In the two-step model, as introduced in sec. 3.2, we provide supervision on the alpha blending mask starting from a factor of 10 for this loss term, and decaying it exponentially with a factor of 0.9997 per weight update, down to 0.01. We observed that this term can be safely decayed without the model becoming unstable or diverging from the expected behavior (i.e. background and foreground separation). This gives G_2 some extra flexibility in drawing details that are not represented by the mask (reflections, shadows).

For the experiments with captions, since COCO comprises five captions per image, we randomly select one caption at training time. In the evaluation phase, we concatenate the representations of all captions since our attention model can easily decide which ones to attend to.

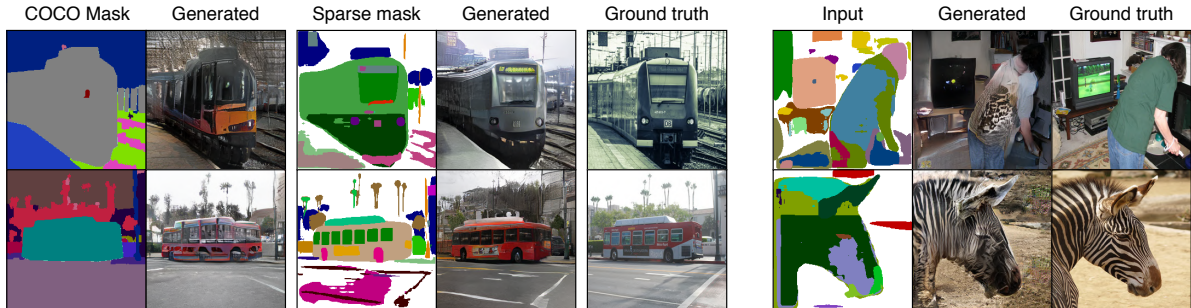


Figure 7: **Left:** the larger set of labels in our sparse masks improves fine details. These masks are easy to obtain with a semi-supervised object detector, and would otherwise be too hard to hand-label. **Right:** some failure cases in our masks, mostly due to noisy detections.

#	Training set	Type	Mask input	Style input	FID
1	COCO-Stuff	1 step [29]	Ground truth	–	22.64
2	COCO-Stuff	1 step	Sparse (ours)	–	20.02
3	COCO-Stuff	1 step	Sparse (ours)	Captions	20.63
4	COCO-Stuff	1 step	Sparse (ours)	Captions+	20.44
5	Visual Genome	1 step	Sparse (ours)	Attributes	21.13
6	Visual Genome	2 steps	Sparse (ours)	Attributes	20.83
7	Visual Genome+	1 step	Sparse (ours)	–	18.93

Table 1: FID scores for different experiments, lower is better. The first line represents the SPADE baseline [29].

4.3. Results

We show the FID scores for various experiments in [Table 1](#). While improving the FID scores is not the goal of our work, it is interesting to see that our weakly-supervised sparse mask setting yields slightly better scores than the supervised baseline (even with an equivalent architecture and training set as in model #2 in the table). We believe that is due to the masks better representing fine details (such as windows, doors, lights, wheels) in compound objects, which are not part of the COCO class set. In [Fig. 7](#) (left) we show a small number of such examples. Furthermore, the experiment on the *augmented* Visual Genome dataset shows that our model benefits from extra unlabeled images (#7). In #4 (*Captions+*), the discriminator is augmented with attributes to provide a stronger supervision signal for the generator. We take the attributes from Visual Genome for the images that overlap between the two datasets. In [Fig. 6](#) we show some qualitative results as well as examples of manipulations, either through attributes or text. Additional examples can be seen in the [Appendix A.3](#), including visualizations of the attention mechanism ([A.4](#)).

As an ablation experiment, in the two-step model (#6) we remove foreground information from the S_{avg} block of the first generator G_1 (we feed the background mask twice in S and S_{avg}). We observe that the FID score increases to 25.16 (from 20.83), meaning that G_1 effectively exploits foreground information to bias the result.

Finally, we observe some failure cases in [Fig. 7](#) (right). Some input masks can be noisy due to imprecise or spurious

detections, leading to incoherent scenes. However, this can be easily tackled by using a better object detector and is not a limitation of our approach. In general, we also observe that our setup tends to work better on outdoor scenes and sometimes struggles with geometric details in indoor scenes or photographs shot from a close range.

5. Conclusion

We introduced a weakly-supervised approach for the conditional generation of complex images. The generated scenes can be controlled through various manipulations on the sparse semantic maps, as well as through textual descriptions or attribute labels. Our results are visually comparable to those of fully-supervised approaches, while enabling a higher level of semantic and style control. From a qualitative point-of-view, we have demonstrated a wide variety of manipulations that can be applied to an image. Furthermore, our weakly supervised setup opens up opportunities for large-scale training on unlabeled datasets, as well as mixed evaluations (training and testing different datasets).

There are several ways one could pursue to further enrich the set of tools used to manipulate the generation process. For instance, the current version of our attention mechanism cannot differentiate between instances belonging to the same class and it also does not have direct access to positional information. Incorporating such information is beyond the scope of this work, but we suggest that this can be achieved by generating queries and values based on *instances* instead of classes, and by appending a *positional embedding* to the query. In the NLP literature, the latter is often learned according to the position of the word in the sentence [39, 7], but images are 2D and therefore do not possess such natural order. Additionally, this would also require captions that are more descriptive than the ones in COCO, which typically focus on actions instead of style. Finally, in order to augment the quality of semantic maps, we would like to train the object detector on a high-quality, large-vocabulary dataset such as [10].

Acknowledgments

This work was partly supported by the Swiss National Science Foundation (SNF) and Research Foundation Flanders (FWO), grant #176004. We would like to thank Graham Spinks and Prof. Sien Moens for helpful discussions.

References

- [1] Andrew Brock, Jeff Donahue, and Karen Simonyan. Large scale GAN training for high fidelity natural image synthesis. In *International Conference on Learning Representations (ICLR)*, 2019. 1, 2, 3
- [2] Holger Caesar, Jasper Uijlings, and Vittorio Ferrari. COCO-Stuff: Thing and stuff classes in context. In *IEEE Conference on Computer Vision and Pattern Recognition (CVPR)*, 2018. 2, 3, 4, 6
- [3] Liang-Chieh Chen, George Papandreou, Iasonas Kokkinos, Kevin Murphy, and Alan L Yuille. Deeplab: Semantic image segmentation with deep convolutional nets, atrous convolution, and fully connected crfs. *IEEE Transactions on Pattern Analysis and Machine Intelligence (TPAMI)*, 40(4):834–848, 2017. 2
- [4] Qifeng Chen and Vladlen Koltun. Photographic image synthesis with cascaded refinement networks. In *IEEE International Conference on Computer Vision (ICCV)*, pages 1511–1520, 2017. 2
- [5] Xinlei Chen, Hao Fang, Tsung-Yi Lin, Ramakrishna Vedantam, Saurabh Gupta, Piotr Dollár, and C Lawrence Zitnick. Microsoft COCO captions: Data collection and evaluation server. *arXiv preprint arXiv:1504.00325*, 2015. 2, 6
- [6] Yu Cheng, Zhe Gan, Yitong Li, Jingjing Liu, and Jianfeng Gao. Sequential attention GAN for interactive image editing via dialogue. *arXiv preprint arXiv:1812.08352*, 2018. 3
- [7] Jacob Devlin, Ming-Wei Chang, Kenton Lee, and Kristina Toutanova. Bert: Pre-training of deep bidirectional transformers for language understanding. *arXiv preprint arXiv:1810.04805*, 2018. 5, 8
- [8] Alaaeldin El-Nouby, Shikhar Sharma, Hannes Schulz, Devon Hjelm, Layla El Asri, Samira Ebrahimi Kahou, Yoshua Bengio, and Graham W. Taylor. Tell, draw, and repeat: Generating and modifying images based on continual linguistic instruction. In *IEEE International Conference on Computer Vision (ICCV)*, 2019. 3
- [9] Ian Goodfellow, Jean Pouget-Abadie, Mehdi Mirza, Bing Xu, David Warde-Farley, Sherjil Ozair, Aaron Courville, and Yoshua Bengio. Generative adversarial nets. In *Neural Information Processing Systems*, pages 2672–2680, 2014. 1
- [10] Agrim Gupta, Piotr Dollar, and Ross Girshick. Lvis: A dataset for large vocabulary instance segmentation. In *IEEE Conference on Computer Vision and Pattern Recognition (CVPR)*, pages 5356–5364, 2019. 8
- [11] Kaiming He, Georgia Gkioxari, Piotr Dollár, and Ross Girshick. Mask R-CNN. In *IEEE International Conference on Computer Vision (ICCV)*, pages 2961–2969, 2017. 7
- [12] Zhenliang He, Wangmeng Zuo, Meina Kan, Shiguang Shan, and Xilin Chen. Attgan: Facial attribute editing by only changing what you want. *IEEE Transactions on Image Processing*, 2019. 1
- [13] Martin Heusel, Hubert Ramsauer, Thomas Unterthiner, Bernhard Nessler, and Sepp Hochreiter. GANs trained by a two time-scale update rule converge to a local Nash equilibrium. In *Neural Information Processing Systems*, pages 6626–6637, 2017. 1, 2, 7
- [14] Tobias Hinz, Stefan Heinrich, and Stefan Wermter. Generating multiple objects at spatially distinct locations. In *International Conference on Learning Representations (ICLR)*, 2019. 3
- [15] Ronghang Hu, Piotr Dollár, Kaiming He, Trevor Darrell, and Ross Girshick. Learning to segment every thing. In *IEEE Conference on Computer Vision and Pattern Recognition (CVPR)*, pages 4233–4241, 2018. 7
- [16] Phillip Isola, Jun-Yan Zhu, Tinghui Zhou, and Alexei A Efros. Image-to-image translation with conditional adversarial networks. In *IEEE Conference on Computer Vision and Pattern Recognition (CVPR)*, pages 1125–1134, 2017. 2, 3
- [17] Justin Johnson, Agrim Gupta, and Li Fei-Fei. Image generation from scene graphs. In *IEEE Conference on Computer Vision and Pattern Recognition (CVPR)*, pages 1219–1228, 2018. 3
- [18] KJ Joseph, Arghya Pal, Sailaja Rajanala, and Vineeth N Balasubramanian. C4Synth: Cross-caption cycle-consistent text-to-image synthesis. In *IEEE Winter Conference on Applications of Computer Vision (WACV)*, pages 358–366. IEEE, 2019. 3
- [19] Tero Karras, Timo Aila, Samuli Laine, and Jaakko Lehtinen. Progressive growing of GANs for improved quality, stability, and variation. In *International Conference on Learning Representations (ICLR)*, 2018. 1, 2
- [20] Tero Karras, Samuli Laine, and Timo Aila. A style-based generator architecture for generative adversarial networks. In *IEEE Conference on Computer Vision and Pattern Recognition (CVPR)*, pages 4401–4410, 2019. 1
- [21] Yannic Kilcher, Aurelien Lucchi, and Thomas Hofmann. Semantic interpolation in implicit models. In *International Conference on Learning Representations (ICLR)*, 2018. 13
- [22] Diederik P Kingma and Max Welling. Auto-encoding variational Bayes. In *International Conference on Learning Representations (ICLR)*, 2014. 1
- [23] Ryan Kiros, Yukun Zhu, Ruslan R Salakhutdinov, Richard Zemel, Raquel Urtasun, Antonio Torralba, and Sanja Fidler. Skip-thought vectors. In *Neural Information Processing Systems*, pages 3294–3302, 2015. 3
- [24] Ranjay Krishna, Yuke Zhu, Oliver Groth, Justin Johnson, Kenji Hata, Joshua Kravitz, Stephanie Chen, Yannis Kalantidis, Li-Jia Li, David A. Shamma, Michael S. Bernstein, and Li Fei-Fei. Visual genome: Connecting language and vision using crowdsourced dense image annotations. *International Journal of Computer Vision (IJCV)*, 123(1):32–73, 2017. 2, 6
- [25] Tsung-Yi Lin, Michael Maire, Serge Belongie, James Hays, Pietro Perona, Deva Ramanan, Piotr Dollár, and C Lawrence Zitnick. Microsoft COCO: common objects in context. In *European Conference on Computer Vision (ECCV)*, pages 740–755. Springer, 2014. 2, 3, 6

- [26] Francesco Locatello, Stefan Bauer, Mario Lucic, Sylvain Gelly, Bernhard Schölkopf, and Olivier Bachem. Challenging common assumptions in the unsupervised learning of disentangled representations. In *International Conference on Machine Learning (ICML)*, 2019. [3](#)
- [27] Takeru Miyato, Toshiki Kataoka, Masanori Koyama, and Yuichi Yoshida. Spectral normalization for generative adversarial networks. In *International Conference on Learning Representations (ICLR)*, 2018. [1](#), [2](#)
- [28] Takeru Miyato and Masanori Koyama. cGANs with projection discriminator. In *International Conference on Learning Representations (ICLR)*, 2018. [1](#), [2](#)
- [29] Taesung Park, Ming-Yu Liu, Ting-Chun Wang, and Jun-Yan Zhu. Semantic image synthesis with spatially-adaptive normalization. In *IEEE Conference on Computer Vision and Pattern Recognition (CVPR)*, pages 2337–2346, 2019. [2](#), [3](#), [4](#), [6](#), [7](#), [8](#), [11](#), [12](#)
- [30] Xiaojuan Qi, Qifeng Chen, Jiaya Jia, and Vladlen Koltun. Semi-parametric image synthesis. In *IEEE Conference on Computer Vision and Pattern Recognition (CVPR)*, pages 8808–8816, 2018. [2](#)
- [31] Scott Reed, Zeynep Akata, Xinchun Yan, Lajanugen Logeswaran, Bernt Schiele, and Honglak Lee. Generative adversarial text to image synthesis. *arXiv preprint arXiv:1605.05396*, 2016. [2](#), [3](#)
- [32] Scott Reed, Aäron van den Oord, Nal Kalchbrenner, Victor Babst, Matt Botvinick, and Nando de Freitas. Generating interpretable images with controllable structure. *OpenReview*, 2016. [3](#)
- [33] Shaoqing Ren, Kaiming He, Ross Girshick, and Jian Sun. Faster R-CNN: Towards real-time object detection with region proposal networks. In *Neural Information Processing Systems*, pages 91–99, 2015. [7](#)
- [34] Shikhar Sharma, Dendi Suhubdy, Vincent Michalski, Samira Ebrahimi Kahou, and Yoshua Bengio. Chatpainter: Improving text to image generation using dialogue. *arXiv preprint arXiv:1802.08216*, 2018. [3](#)
- [35] Karen Simonyan and Andrew Zisserman. Very deep convolutional networks for large-scale image recognition. *arXiv preprint arXiv:1409.1556*, 2014. [4](#)
- [36] Krishna Kumar Singh, Utkarsh Ojha, and Yong Jae Lee. FineGAN: Unsupervised hierarchical disentanglement for fine-grained object generation and discovery. In *IEEE Conference on Computer Vision and Pattern Recognition (CVPR)*, 2019. [3](#), [4](#), [6](#)
- [37] Rupesh Kumar Srivastava, Klaus Greff, and Jürgen Schmidhuber. Highway networks. In *ICML Deep Learning Workshop*, 2015. [6](#)
- [38] Christian Szegedy, Vincent Vanhoucke, Sergey Ioffe, Jon Shlens, and Zbigniew Wojna. Rethinking the inception architecture for computer vision. In *IEEE Conference on Computer Vision and Pattern Recognition (CVPR)*, pages 2818–2826, 2016. [3](#)
- [39] Ashish Vaswani, Noam Shazeer, Niki Parmar, Jakob Uszkoreit, Llion Jones, Aidan N Gomez, Łukasz Kaiser, and Illia Polosukhin. Attention is all you need. In *Neural Information Processing Systems*, pages 5998–6008, 2017. [3](#), [5](#), [8](#)
- [40] Ting-Chun Wang, Ming-Yu Liu, Jun-Yan Zhu, Andrew Tao, Jan Kautz, and Bryan Catanzaro. High-resolution image synthesis and semantic manipulation with conditional GANs. In *IEEE Conference on Computer Vision and Pattern Recognition (CVPR)*, pages 8798–8807, 2018. [2](#), [3](#), [4](#), [11](#)
- [41] Tao Xu, Pengchuan Zhang, Qiuyuan Huang, Han Zhang, Zhe Gan, Xiaolei Huang, and Xiaodong He. AttnGAN: Fine-grained text to image generation with attentional generative adversarial networks. In *IEEE Conference on Computer Vision and Pattern Recognition (CVPR)*, pages 1316–1324, 2018. [2](#), [3](#), [5](#)
- [42] Xinchun Yan, Jimei Yang, Kihyuk Sohn, and Honglak Lee. Attribute2image: Conditional image generation from visual attributes. In *European Conference on Computer Vision (ECCV)*, pages 776–791. Springer, 2016. [1](#)
- [43] Jianwei Yang, Anitha Kannan, Dhruv Batra, and Devi Parikh. LR-GAN: layered recursive generative adversarial networks for image generation. In *International Conference on Learning Representations (ICLR)*, 2017. [3](#), [4](#), [6](#)
- [44] Guojun Yin, Bin Liu, Lu Sheng, Nenghai Yu, Xiaogang Wang, and Jing Shao. Semantics disentangling for text-to-image generation. In *IEEE Conference on Computer Vision and Pattern Recognition (CVPR)*, pages 2327–2336, 2019. [3](#)
- [45] Han Zhang, Ian Goodfellow, Dimitris Metaxas, and Augustus Odena. Self-attention generative adversarial networks. In *International Conference on Machine Learning (ICML)*, 2019. [1](#), [2](#), [3](#)
- [46] Han Zhang, Tao Xu, Hongsheng Li, Shaoting Zhang, Xiaogang Wang, Xiaolei Huang, and Dimitris N Metaxas. StackGAN: Text to photo-realistic image synthesis with stacked generative adversarial networks. In *IEEE International Conference on Computer Vision (ICCV)*, pages 5907–5915, 2017. [2](#), [3](#), [5](#), [13](#)
- [47] Han Zhang, Tao Xu, Hongsheng Li, Shaoting Zhang, Xiaogang Wang, Xiaolei Huang, and Dimitris N Metaxas. StackGAN++: Realistic image synthesis with stacked generative adversarial networks. *IEEE Transactions on Pattern Analysis and Machine Intelligence (TPAMI)*, 41(8):1947–1962, 2018. [2](#), [3](#), [5](#)
- [48] Bo Zhao, Lili Meng, Weidong Yin, and Leonid Sigal. Image generation from layout. In *IEEE Conference on Computer Vision and Pattern Recognition (CVPR)*, pages 8584–8593, 2019. [3](#)
- [49] Jun-Yan Zhu, Taesung Park, Phillip Isola, and Alexei A Efros. Unpaired image-to-image translation using cycle-consistent adversarial networks. In *IEEE International Conference on Computer Vision (ICCV)*, pages 2223–2232, 2017. [2](#), [3](#)

A. Supplementary material

A.1. Detailed architecture

In this section, we provide additional implementation details about our architecture in order to consolidate the already-presented Fig. 3 (overview of the generators), Fig. 4 (S and S_{avg} blocks), and Fig. 5 (attention mechanism for image captions).

One-step generator. In sec. 3.2 we mention that the backbone of the one-step model is the same as [29], and that we only modify the SPADE normalization blocks as well as the very first layer of the generator. In Fig. 8a we show the detailed architecture of this model. The implementation of an individual “SPADE ResBlock” is specified in [29], but for reference we mention that each residual block consists of two SPADE normalization blocks wrapped by a skip-connection. If the number of input and output channels does not match, the skip-connection is learned, i.e. we learn a third SPADE normalization block. In the models conditioned on captions, we never attach attention inputs to skip-connections (to avoid potential instabilities). Each normalization block learns its own set of weights, and in our case they correspond to the S or S_{avg} blocks specified in Fig. 4.

It is worth noting that, in the SPADE reference implementation, the input layer can either take a noise vector (for generation using a style image) or the semantic map as input. Since we control style deterministically, we are only interested in the latter case, so we simply concatenate style information to the semantic map in the same way as we do it in an S block. This also applies to the *two-step* model.

Two-step generator. The architecture of the two-step generator is depicted in Fig. 9, and differs significantly from the aforementioned implementation. The background generator G_1 is a simplified version of the one-step generator with fewer residual blocks. The foreground generator G_2 implements a bottleneck architecture that takes as input the generated background image and compresses it through a series of *non*-SPADE residual blocks. The low-resolution feature-map is then expanded again through a series of SPADE residual blocks. Interestingly, for foreground manipulations it is possible to preprocess the feature maps up to the last downsampling block in G_2 (8×8 resolution) and greatly speed up regeneration.

Discriminator. We use the multi-scale discriminator from [40, 29] and change its input layer to add information about attributes or captions. The architecture is shown in Fig. 8b. As usual with multi-scale discriminators, we train two instances: one which takes as input an image with full resolution, and one which takes as input a downsampled version (by a factor of two). They learn a different set of embeddings, and a different set of attention heads if the style is conditioned on a sentence.

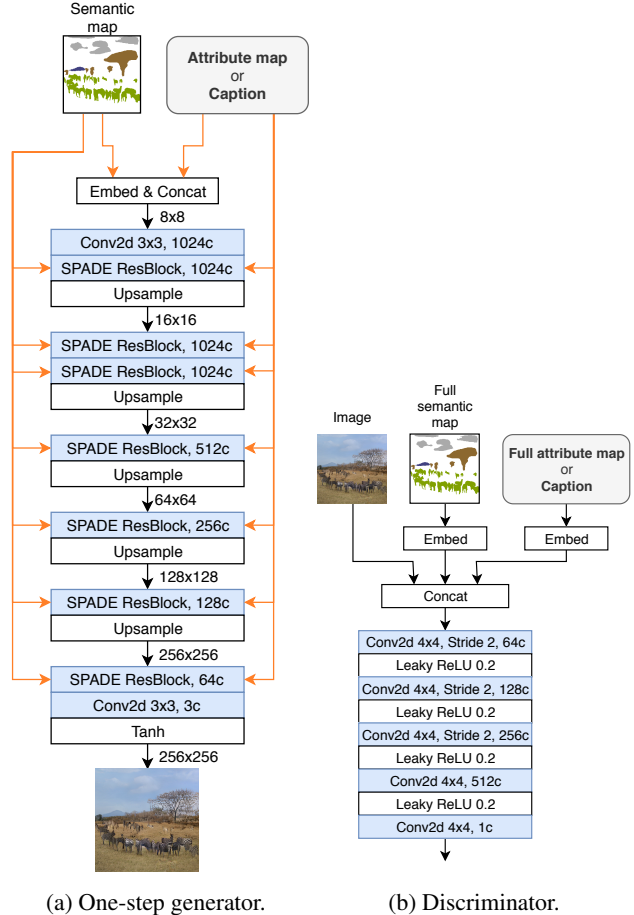


Figure 8: **(a)** One-step generator, equivalent to [29] except for the input layer and SPADE normalization blocks. “1024c” stands for “1024 output channels”. The number on the right of an arrow specifies the feature map resolution at that level. Orange arrows indicate that the input information is fed to S blocks. **(b)** Discriminator (used in all architectures), again equivalent to [29] except for the input layer.

Model complexity. Table 2 presents the number of parameters for all variants of our approach. The SPADE baseline trained on the 182 COCO-Stuff classes requires 97.5M parameters. Our 1-step baseline trained without style information (neither attributes nor captions) on our set of 280 classes requires a slightly lower number of parameters (94.2M). As explained in sec. 3.2, this is due to replacing 3×3 convolutions over one-hot vectors with point-wise 64-dim embeddings followed by 3×3 convolutions. In the version with attributes, the added cost (+2.3M parameters) is only due to the learned attribute embeddings (256 64-dim embeddings per SPADE normalization block). In the version with captions, the custom attention modules add a significant cost (+23.3M parameters), but this can be easily reduced by training fewer attention heads (e.g. 6 instead of

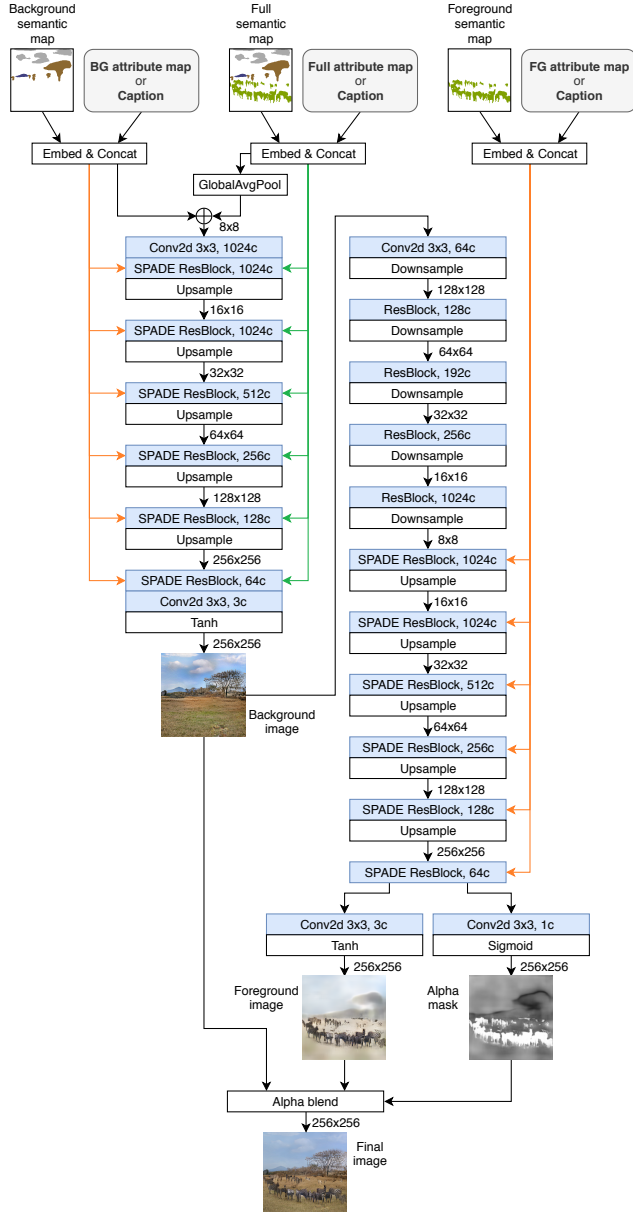


Figure 9: Two-step generator. The left side of the figure depicts G_1 (background generator), while the right side depicts G_2 (foreground generator). Orange arrows indicate that the input information is fed to S blocks, whereas green arrows denote inputs to S_{avg} blocks.

the default 12).

We conduct a similar analysis for the two-step model. In this case, the background generator is slightly more powerful than the foreground generator.

Semantic map generation. In this paragraph we provide further details in addition to those presented in [sec. 4.2](#). Specifically, we describe how we construct and maintain the data structure that enables instance manipulation and raster-

Approach	Style input	# params
Baseline [29]	None	97.5M
1-step	None	94.2M
1-step	Attributes	96.5M
1-step	Captions	117.5M
2-step	None	74.5M + 50.6M
2-step	Attributes	78.3M + 51.9M
2-step	Captions	90.7M + 65.8M

Table 2: Number of parameters for different variations of our approach. For the two-step models we specify the numbers for both generators (respectively G_1 and G_2).

ization. Since a scene may consist of objects that partially overlap, the order in which they are drawn on the semantic map is important, e.g. given a *car* and its *headlight*, we want to render the headlight semantic mask on top of the car and not the opposite. Therefore, we sort all instances by mask area and draw them from the largest to the smallest. Additionally, we construct a hierarchical structure to facilitate manipulation: if 70% of the area of an instance is contained within another instance, it becomes a child of the latter. With regard to the previous example, moving the car would also move the headlights attached to it. This hierarchy is only used for manipulation purposes, and has no effect on the model. Finally, in our experiments on Visual Genome, we link attributes to an instance if the IoU between the ground-truth region and the detected bounding box is greater than 0.5.

A.2. FID evaluation

The FID metric is very sensitive to aspects such as image resolution, number of images (where a low number results in worse FID scores), and the weights of the pretrained Inception network. To be consistent with [29], we try to follow their methodology as closely as possible. We resize the ground-truth images to the same resolution as the generated ones (256×256), and we keep the two sets aligned, i.e. one generated image per test image. We use the weights of the pretrained InceptionV3 network provided by PyTorch. To make the results in [Table 1](#) comparable, we retrained the baseline from [29] and evaluated the results using our methodology.

A.3. Additional results

[Fig. 11](#) and [Fig. 12](#) show examples of semantic manipulation and style manipulation (either using attributes or text). The last row of [Fig. 12](#) suggests that our attention mechanism can correctly exploit the contextualized token embeddings produced by BERT. For instance, the caption “a black and white cat” affects only the cat, while “a black and white picture of a cat” affects the entire scene by generating a black-and-white image.

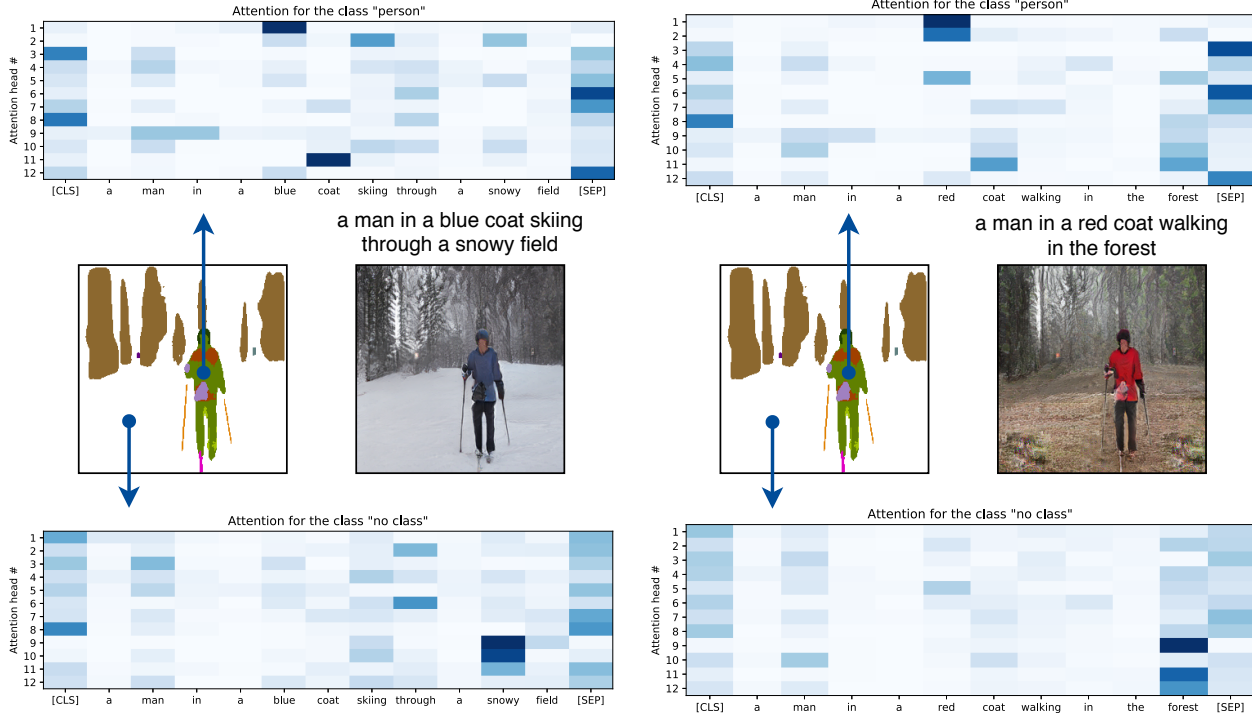


Figure 10: Visualization of the attention mechanism in the discriminator for two images generated from the same semantic map, but different captions. An attention map is produced for each class in the semantic map, and each of these consists of 12 independent attention heads. In this illustration we only show those corresponding to *person* and *no class* (i.e. blank space). [CLS] and [SEP] are special delimiters indicating respectively the start and end of a sentence. A head paying attention to these can be interpreted as not being triggered by the sentence. In the attention maps, a darker color indicates a higher weight.

Fig. 13 shows additional demos generated by our two-step model on the Visual Genome development set. In particular, we highlight the decomposition of the background and foreground, and the inputs taken by G_1 and G_2 . Since G_2 outputs a soft transparency channel for the alpha blending, it can slightly violate the constraints imposed by the *foreground mask*. This allows it to draw reflections and shadows underneath foreground objects.

A.4. Attention visualization

The behavior underlying our attention model can be easily visualized. Our formulation (*sentence-semantic* attention) is particularly suited for visualization tasks because it is tied to the semantic map, and not to feature maps in inner convolutional layers. Therefore, for each class in the semantic map (e.g. *person*, *tree*, *empty space*), we can observe how the sentence conditions that particular class.

Considering that the attention modules have multiple entry points in the generator (one for each SPADE normalization block), it is easier to carry out this analysis in the discriminator, where there are only two entry points (in the input layer of each discriminator, since we adopt a multi-scale discriminator). We select the first discriminator for illus-

tration purposes, and show the resulting attention maps in Fig. 10. The figure shows what parts of the sentence the discriminator is attending to in order to discriminate whether the caption is suitable for the input image.

A.5. Demo video and interpolation

The accompanying video in the supplementary material shows some examples of interactive manipulations. Among other things, we show that our approach can smoothly interpolate between masks, attributes, and text. While attention models usually preclude interpolation (whereas models based on fixed-length sentence embeddings such as [46] easily allow it), our *sentence-semantic* attention mechanism enables interpolation over the *contextualized class embeddings*, i.e. over the pooled attention values. For all cases (masks, attributes, text), we respectively interpolate between class embeddings, attribute embeddings, and contextualized class embeddings using spherical interpolation (*slerp*), which traverses regions with a higher probability mass [21]. Unlike [46], we found it unnecessary to enforce a prior on the embeddings via a KL divergence term in the loss.



Figure 11: Examples of semantic and attribute manipulations (Visual Genome dataset). The images are generated by our two-step model. In the first row, the background is frozen to encourage locality.



Figure 12: Further examples of style manipulation using text (COCO2017 validation set). It is possible to control the style of individual instances (albeit in a less targeted fashion than attributes) as well as the global style of the image.



Figure 13: Demos generated by our two-step model. In addition to the full input mask, we show its decomposition into *background mask* and *foreground mask* (taken as input in S blocks respectively by G_1 and G_2). Note that G_1 also takes as input the full mask in S_{avg} blocks.